Ceramics-Silikáty 61 (1), 34-39 (2017)
journal webpage: www.ceramics-silikaty.cz doi: 10.13168/cs.2016.0057

PREPARATION AND EVALUATION OF THE COLOR PROPERTIES OF $YFeO_3$ PIGMENTS DOPED BY In^{3+} AND Ga^{3+}

#ANETA BURKOVIČOVÁ, ŽANETA DOHNALOVÁ, PETRA ŠULCOVÁ

Department of Inorganic Technology, Faculty of Chemical Technology, University of Pardubice, Studentská 95, 532 10 Pardubice, Czech Republic

#E-mail: aneta.burkovicova@student.upce.cz

Submitted March 31, 2016; accepted October 13, 2016

Keywords: Inorganic pigments, CIE color system, X-ray diffractometry, Thermal analysis (DTA, TG), Yttrium iron oxide

Inorganic pigments of type $YFe_x(M)_{1-x}O_3$, where M = In or Ga and x = 1 or 0.95, were synthesized by mechanical activation in liquid medium (H_2O + C_2H_6O) and successive two-step heating in the range 900 - 1300°C. TG-DTA analysis of a mixture of starting oxides Fe_2O_3 and Y_2O_3 was performed in order to compare the thermal behavior of reagents before and after mechanical activation. $YFeO_3$ was prepared as a standard and applied into the ceramic glaze and acrylic copolymer matrix (mass and diluted tone). Samples were characterized by XRD analysis, particle size distribution (PSD) and color measurements. The effect of substitution of 5 mol. % Fe^{3+} for In^{3+} or Ga^{3+} on the changes of pigment properties was examined.

INTRODUCTION

$YFeO_3$ belongs to the group of rare-earth orthoferrites with general formula $RFeO_3$ (R represents a trivalent rare-earth ion) and perovskite-type structure. They attract attention primarily thanks to their magnetic and optic properties, which were described for the first time by Forestier and Guit-Guillaind in 1950 [1]. These materials are also characterized by excellent catalytic activity depending on factors as surface area, pore structure, oxygen nonstoichiometry, reducibility and also for their high activity, structural stability and resistance to the catalyst poisons especially in the automotive industry [2-5]. Pure $YFeO_3$ is a p-type indirect semiconductor with a band gap of 2.58 eV, which is slightly wider than the band gap of Fe_2O_3. Therefore it is a suitable candidate for water-splitting under visible light [6, 7].

$YFeO_3$ crystallizes in a distorted perovskite structure with an orthorhombic unit cell. The distortion from the ideal perovskite is caused by the position of the R^{3+} ions while the position of Fe^{3+} ions remains octahedral. $YFeO_3$ can also crystallize in a metastable hexagonal ($YAlO_3$-type) structure depending on synthesis conditions. Research has revealed that this perovskite is thermodynamically unstable and impurity phases Fe_3O_4 or $Y_3Fe_5O_{12}$ (Yttrium Iron Garnet – YIG) are often created during high-temperature synthesis. That makes the preparation of single-phased perovskite $YFeO_3$ a complex task [4, 8-14]. Numbers of reports are available on $YFeO_3$ synthesis like sol–gel, microwave-assisted, self-propagating combustion synthesis, solid state reaction, alkoxide method, sonochemical synthesis, pulsed laser deposition, combustion or hydrothermal techniques, precipitation method, thermal decomposition, solvothermal treatment, Pechini method etc. followed by high-temperature calcination [4, 7, 10, 15-18]. $YFeO_3$ has possible practical applications in catalysts, gas-sensitive sensors (registered as a photocatalyst for CO oxidation, explored for photocatalytic oxidation of organic dyes and the selective catalytic reduction of NO_x to N_2 by propene), optical switches, magneto-optical current sensors, cathodes in solid oxide fuel cells, environmental monitoring films, data storage devices, detectors of humidity and alcohols and material for magnetic resonance imaging (MRI) in biomedicine [4, 6, 7, 9, 11, 15, 19 - 21].

One of the few studies that explore the possibility of using $YFeO_3$ as an inorganic pigment is a study of $YMn_xFe_{1-x}O_3$ prepared by a modified citrate method [22]. The color of the prepared samples is changing from blue-green to dark blue. Moreover, the chromatic properties NIR reflectance and thermal stability were investigated and the phase composition was examined by XRD analysis.

The aim of our research was to verify the possibility of $YFe_xM_{1-x}O_3$ (M = In or Ga; x = 1 or 0.95) preparation and to investigate changes of pigment properties depending on composition and calcination temperature. Samples were prepared by mechanical activation in a liquid medium and pigment properties such as particle size distribution, phase composition and color properties were studied.

EXPERIMENTAL

The pigments $YFe_xM_{1-x}O_3$, where M = In of Ga and x = 1 or 0.95, were prepared by mechanical activation in liquid medium (volume ratio H_2O:C_2H_6O = 1:1). Reagents Y_2O_3 (99.99 % purity, Alfa Aesar, Germany), Fe_2O_3 (99 % purity, Precheza, Czech Republic); Ga_2O_3 (99.99 % purity, Alfa Aesar, Germany) or In_2O_3 (99.5 % purity, Alfa Aesar, Germany) were weighed in selected proportions and homogenized in a mortar. The prepared mixtures were milled in a planetary mill (Pulverisette 5, Fritsch, Germany) for 5 hours. The mass ratio of pigment and agate milling balls was 1:8.2 and as a liquid medium mixture of deionized water and ethanol in the volume ratio 1:1 was used. Powders were subsequently dried and re-homogenized. The reaction mixtures were fired in an electric furnace at 700°C with a soaking time of 6 hours in the first step and in the second step in the range 900 - 1300°C (also for 6 hours). The pigments were applied in an organic matrix (urethane-acrylate copolymer Parketol, Balacom, Czech Republic) in mass and diluted tone. The mass tone denotes the color obtained when the pigmented medium is applied as a layer on a white substrate. In the diluted tone pigmented medium consist of a mixture of the pigment and TiO_2 in the weight ration 1:1. Pigments were applied in a ceramic glaze (G028 91, Glazura, Czech Republic) as well. The mixture of pigment in amounts of 10 wt. % and glaze was glazed at 900°C for 15 min. The applications of pigments in the organic matrix and ceramic glaze were evaluated by measuring the spectral reflectance in the visible region of light (400 - 700 nm) using a ColorQuest XE (HunterLab, USA). Illuminant D65 (standardized light simulating daylight), measuring geometry *d*/8° and 10° complementary observer (i.e. the sample is illuminated by diffuse light coming from an integrating sphere and the detection angle is 8° and 10° off the normal) were used as the measuring conditions. The color properties were described in the most common color system - the CIE system *L*a*b** [23]. The values *a** (the red-green axis) and *b** (the yellow-blue axis) indicate the hue. The value *L** represents the lightness or darkness of the color. *L** is ranging from 0 (black) to 100 (white). From the previous values it is possible to calculate the *C* value (chroma), the hue angle H° and the color difference ΔE* according to the formulas:

$$C = (a^{*2} + b^{*2})^{1/2}, \quad (1)$$

$$H° = \text{arc tg}\,(b^*/a^*), \quad (2)$$

$$\Delta E^* = [(\Delta L^*)^2+(\Delta a^*)^2+(\Delta b^*)^2]^{1/2}. \quad (3)$$

The C value represents the saturation of the color and the hue angle *H*° expresses the color using an angular position in the cylindrical color space (*H*° = 350-35° = = red, *H*° = 35-70° = orange, *H*° = 70-105° = yellow, *H*° = 105-195° = green, *H*° = 195-285° = blue and *H*° = 285-350° = violet). ΔE* is the color difference between standard and sample. The difference is perceptible when ΔE* is in the range from 1.5 to 3. If it is greater than 3, then the change of the color is significant.

The particle size distribution (PSD) was measured using a Mastersizer 2000/MU (Malvern Instruments, UK) which operates on the principle of diffraction of light on particles dispersed in a liquid medium (mixture of 800 ml of deionised water and 4.8 ml of $Na_4P_2O_7$ solution with a concentration of 3 $g{\cdot}l^{-1}$). As the source of light a He-Ne laser (wavelength 633 nm) and a blue light diode laser (466 nm) were used. The samples were ultrasonically homogenized for 90 s in a solution of $Na_4P_2O_7$ (0.15 $g{\cdot}l^{-3}$) and added to the dispersing liquid in an amount at which the laser obscuration caused by the pigment particles reaches the level 12.5 %. The software evaluates the PSD based on the Fraunhofer approximation.

The crystal structure was verified using a diffractometer Empyrean (PANalytical, Netherlands) with vertical goniometer (step size 0.0001°) and 2θ geometry (10 - 100°). A copper anode is used as a source of X-ray radiation and a photon counting detector for the registration of X-ray photons.

Thermal analysis was carried out for reaction mixtures before and after mechanical activation. The aim was to determine the effect of treatment in the planetary mill on the chemical reactions in the system. Simultaneous TG-DTA measurements were performed by 449C Jupiter (Netzsch, Germany) in the temperature range 30 - 1300°C with heating rate 10°C min^{-1} in air atmosphere.

RESULTS AND DISCUSSION

A record of simultaneous TG-DTA measurements of a $YFeO_{3\pm\delta}$ sample before mechanical activation (sample weight = 307.3 mg) is illustrated in Figure 1a. Three endothermic peaks and one exothermic peak are seen on the DTA curve. The endothermic peak with the minimum at 410°C is attributed to decomposition of $Y_2(CO_3)_3$ which is formed by reaction of Y_2O_3 and CO_2 when the oxide is kept in air atmosphere [24]. It is accompanied by a weight loss on the TG curve of 0.7 %. The following two endothermic peaks are related to the phase transition α-Fe_2O_3 to β-Fe_2O_3 (peak with a minimum at 680°C) and further to γ-Fe_2O_3 at 783°C [25]. The exothermic peak with maximum at 1047°C is attributed to the gradual formation of crystalline $YFeO_3$ [26].

Figure 1b shows the results of thermal analysis of the sample after mechanical activation (sample weight = 306.1 mg). This mixture is stable up to temperature of 850°C. The first and second exothermic peak with maxima at 904 and 982°C are associated with the gradual formation of the perovskite structure. At the same time, the TG curve decreases due to the loss of oxygen in the

system and decomposition of $Y_2(CO_3)_3$ (weight loss of about 2 %). In the temperature range 1000 - 1100°C Y_3FeO_{12} is formed. Its amount is very small and the formation is not accompanied by significant changes in the DTA curve. The endothermic peak with a minimum at 1250°C is attributed to partial melting and sintering of the sample. Thermal analysis confirmed that perovskite phase is formed in the temperature range 900 - 1000°C and that the method of preparation has a major influence on the reactions in the system during the first stage of the heat treatment.

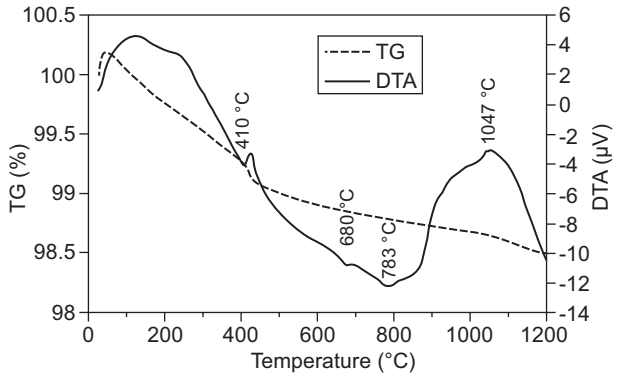

a)

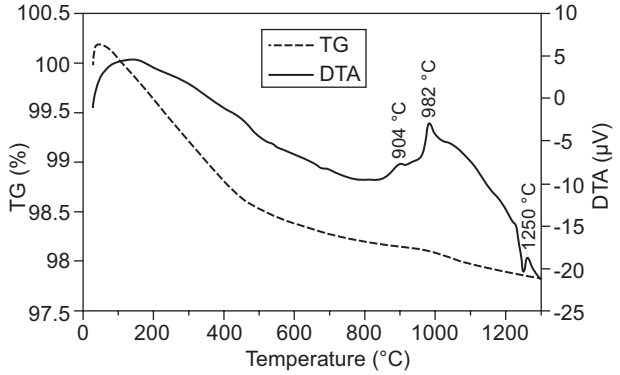

b)

Figure 1. TG-DTA analysis of mixtures of starting oxides before (a) and after (b) mechanical activation.

The phase composition of all samples was verified by X-ray diffraction analysis. At 900°C the system of standard $YFeO_{3\pm\delta}$ still contains non-reacted starting oxides Y_2O_3 (PDF No. 00-041-1105) [27], although the Fe_2O_3 (PDF No. 01-079-1741) and desired product $YFeO_3$ (PDF No. 01-086-0170) is created as well. At 1000°C the sample is still not fully reacted, but the amount of $YFeO_3$ has increased. Both expected products are created during calcination at 1100°C: $YFeO_3$ (PDF No. 01-086-0170) and thermally more stable $Y_3Fe_5O_{12}$ (PDF No. 00-043-0507). However, the sample still contains a small amount of Y_2O_3. The system is completely reacted at 1200°C and even after increasing firing temperature to 1300°C (Figure 2a) there are no more changes in the composition of this sample.

The phase composition of the sample doped by Ga^{3+} ions is similar to the previous standard. The system is fully reacted at 1200°C when $YFeO_3$ (PDF No. 01-086-0170) and $Y_3Fe_5O_{12}$ (PDF No. 00-043-0507) are created. The structure does not change even when the temperature rises to 1300°C. In comparison with the standard sample the pigment $YFe_{0.95}Ga_{0.05}O_{3\pm\delta}$ contains a larger amount of $Y_3Fe_5O_{12}$ (Figure 2b).

In the case of $YFe_{0.95}In_{0.05}O_{3\pm\delta}$ the course of reactions is slightly different. At 900°C the sample contains, apart from of Y_2O_3 and Fe_2O_3, the product $YFeO_3$ and the by-product Fe_2O_3 (PDF No. 99-100-8126). Increasing the firing temperature causes a successive consumption of the starting oxides and the by-product for the formation of $YFeO_3$ and $Y_3Fe_5O_{12}$, but Y_2O_3 remains in the system even after firing at 1300°C. In addition, from a shift of the diffraction peaks it is evident that In^{3+} ions are replacing Y^{3+} in $YFeO_3$ instead of Fe^{3+}. In^{3+} is also built into $Y_3Fe_5O_{12}$ to form a compound structurally equivalent to $Y_3In_{0.42}Fe_{4.58}O_{12}$ (PDF No. 01-071-0099). The improper substitution is caused probably due to the bigger ionic radius of In^{3+} (0.80 Å) compared to Fe^{3+} (0.64 Å). For In^{3+} ions it is thus easier to substitute Y^{3+} with ionic radius 1.07 Å instead.

The color properties of the standard pigment $YFeO_{3\pm\delta}$ are shown in Table 1. In mass tone the value

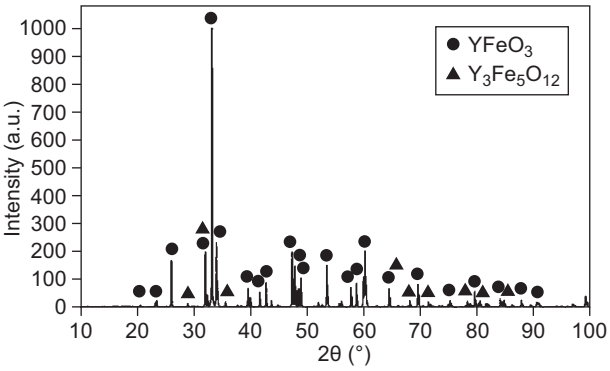

a)

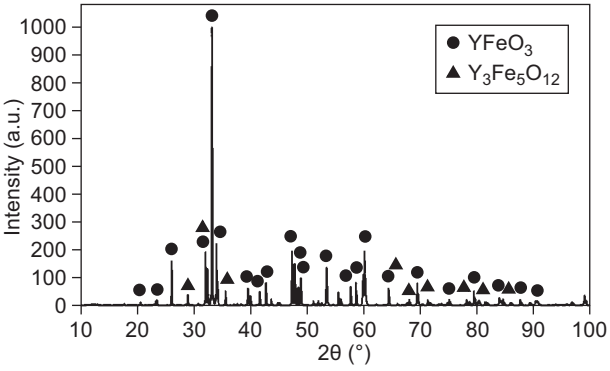

b)

Figure 2. Diffractograms of pigments $YFeO_{3\pm\delta}$ (a) and $YFe_{0.95}Ga_{0.05}O_{3\pm\delta}$ (b) fired at 1300°C.

of the red axis a* decreases with rising temperature. The highest content of red color has sample fired at 900°C because of non-reacted Fe_2O_3. The yellow coordinate b* increases up to 1100°C where it reaches its maximum value (24.40). This sample is also the lightest due to highest lightness value (L* = 43.19). At higher temperatures the pigment loses not only the yellow color but also brightness and chroma. The color of this application changes from red to brownish yellow and dark brown. The values of color coordinates in diluted tone have a similar sequence. The a* value decreases with rising temperature and opposite the b* value increases to the 1100°C. Application of the sample prepared at 1300°C is considerably lighter and its hue is without significant contribution of any color which may be caused by the larger particle size. The color is shifting from pink to light yellow with rising temperature.

Table 2 demonstrates the influence of calcination temperature on the color properties of the $YFe_{0.95}In_{0.05}O_{3\pm\delta}$ pigment. By doping with In^{3+} ions a highlighting of both red and yellow color was achieved. The biggest color difference between the standard $YFeO_{3\pm\delta}$ and the $YFe_{0.95}In_{0.05}O_{3\pm\delta}$ sample is manifested for the pigment fired at 1300°C (ΔE* = 20.04). On the other hand, the smallest difference was measured for the pigment fired at 1000°C. ΔE* (1.83) is in this case in the region of almost imperceptible difference. With increasing temperature the color is changing from red to yellowish brown and dark brown. After application in diluted tone higher values of a* and b* were measured, opposite to the standard $YFeO_3$. Their hue is slightly more saturated and the chroma value (C) decreases with increasing temperature very slightly. ΔE* values are in the range 3.5 - 12 which indicate a significant color difference. The hue of these pigments varies from pink to pale yellowish brown.

The values of color coordinates of pigments doped by 5 mol. % Ga^{3+} are shown in Table 3. The results are very similar to the samples doped by In^{3+} ions. After application in mass tone pigments with higher values of the yellow and red coordinates were obtained. The a* value alternately increases and decreases with increasing temperature but b* rises up to 1200°C. This sample has also the highest chroma (C = 36.10). The color differences ΔE* (standard $YFeO_{3\pm\delta}$; sample $YFe_{0.95}Ga_{0.05}O_{3\pm\delta}$) are more pronounced at higher temperatures and the largest difference was measured again for the application of the pigment calcined at 1300°C. Samples in diluted tone exhibit a similar trend. The content of red color also decreases with increasing temperature, and yellow hue dominates in these samples. The pigment doped by Ga^{3+} and fired at 1300°C is brighter, has a lower content of red and yellow and also is less saturated than the In^{3+} doped one. Shades are changing from pink to light brown.

Table 1. Color properties of pigment $YFeO_{3\pm\delta}$ applied to the organic matrix in mass and diluted tone.

T [°C]	mass tone					diluted tone				
	L*	a*	b*	C	H°	L*	a*	b*	C	H°
900	38.51	20.00	12.37	23.52	31.74	54.06	17.47	7.85	19.15	24.20
1000	41.66	17.11	18.10	24.91	46.61	59.79	12.56	10.81	16.57	40.72
1100	43.19	17.08	24.40	29.78	55.01	66.10	10.28	14.21	17.54	54.12
1200	38.64	17.25	19.63	26.13	48.69	66.01	9.20	7.33	11.76	38.55
1300	34.52	12.53	10.32	16.23	39.48	71.45	5.77	4.30	7.20	36.69

Table 2. Color properties of pigment $YFe_{0.95}In_{0.05}O_{3\pm\delta}$ applied to the organic matrix in mass and diluted tone.

T [°C]	mass tone						diluted tone					
	L*	a*	b*	C	H°	ΔE*	L*	a*	b*	C	H°	ΔE*
900	39.37	22.47	13.28	26.10	30.58	2.77	53.64	20.17	10.13	22.57	26.67	3.56
1000	41.80	18.70	17.21	25.41	42.62	1.83	60.04	14.62	13.56	19.94	42.85	3.45
1100	47.32	18.28	28.76	34.08	57.56	6.12	69.29	11.18	19.18	22.20	59.76	5.97
1200	46.61	20.56	28.68	35.29	54.36	12.51	69.03	12.58	17.82	21.81	54.78	11.43
1300	43.47	22.23	25.40	33.75	48.81	20.04	69.81	12.44	14.02	18.74	48.42	11.90

Table 3. Color properties of pigment $YFe_{0.95}Ga_{0.05}O_{3\pm\delta}$ applied to the organic matrix in mass and diluted tone.

T [°C]	mass tone						diluted tone					
	L*	a*	b*	C	H°	ΔE*	L*	a*	b*	C	H°	ΔE*
900	39.40	23.24	13.47	26.86	30.10	3.54	54.63	20.82	9.76	22.99	25.12	3.90
1000	41.61	19.21	17.01	25.66	41.52	2.37	58.52	14.67	11.61	18.71	38.36	2.59
1100	47.04	16.65	27.44	32.10	58.75	4.92	67.34	10.18	19.30	21.82	62.19	5.24
1200	47.64	20.46	29.74	36.10	55.47	13.91	70.45	11.48	17.58	21.00	56.85	11.40
1300	42.30	19.72	22.58	29.98	48.87	16.20	72.00	10.40	12.42	16.20	50.06	9.36

Table 4. Color properties of pigments $YFeO_{3\pm\delta}$; $YFe_{0.95}In_{0.05}O_{3\pm\delta}$ and $YFe_{0.95}Ga_{0.05}O_{3\pm\delta}$ applied to a ceramic glaze of type G 02891.

T [°C]	$YFeO_{3\pm\delta}$			$YFe_{0.95}In_{0.05}O_{3\pm\delta}$				$YFe_{0.95}Ga_{0.05}O_{3\pm\delta}$			
	L*	C	H°	L*	C	H°	ΔE*	L*	C	H°	ΔE*
900	36.97	10.31	33.37	36.53	11.75	24.65	2.25	34.92	12.91	28.61	3.44
1000	36.72	9.13	30.55	36.47	9.94	28.21	0.94	35.74	10.59	26.40	1.90
1100	37.66	11.82	33.19	37.21	11.71	30.59	0.71	37.31	11.39	32.67	0.56
1200	37.77	13.06	30.67	38.25	14.38	34.29	1.65	38.15	14.23	33.59	1.41
1300	37.08	14.28	32.62	36.25	16.14	35.14	2.14	37.53	14.64	33.86	0.66

Table 5. Particle size distribution (PSD) of prepared pigment powders.

T [°C]	$YFeO_{3\pm\delta}$			$YFe_{0.95}In_{0.05}O_{3\pm\delta}$			$YFe_{0.95}Ga_{0.05}O_{3\pm\delta}$		
	d_{10}	d_{50}	d_{90}	d_{10}	d_{50}	d_{90}	d_{10}	d_{50}	d_{90}
900	0.6	1.8	5.2	0.4	1.3	5.2	0.4	1.3	4.1
1000	0.7	2.7	6.7	0.5	1.7	5.0	0.5	1.6	4.4
1100	1.0	3.5	8.3	0.6	2.7	7.2	0.5	2.4	5.8
1200	1.6	4.6	19.0	0.7	3.0	7.0	0.6	2.7	6.9
1300	1.8	5.9	36.0	1.1	3.4	8.4	1.1	3.8	16.3

The pigments were also applied in a ceramic glaze of type G028 91 (transparent ceramic glaze, Glazura, Torrecid Group, Czech Republic). Values L*, C, H° and ΔE* are shown in Table 4. The results for all samples are rather similar. Their color is reddish brown and does not depend on the composition or calcination temperature. The values of color coordinates are lower than for application in mass tone, which corresponds to lower chroma values C. The hue angles of all pigments are in the red region and the color difference ΔE* does not exceed the level of 3.44. These samples are probably not stable in the aggressive environment of the molten glaze, and thus differences between the individual pigments are becoming minimal.

Another important parameter in the evaluation of pigment properties is the particle size distribution (PSD). The most important value is the median size d_{50}, but for the general description of the system it is common practice to cite also d_{10} and d_{90}. PSD results are listed in Table 5. With increasing temperature the d_{50} values rise for all pigments. The median size of standard $YFeO_3$ ranges from 1.8 to 5.9 μm. The sample fired at 1300°C was partially sintered as is evident from the high d_{90} value (36 μm). Doped pigments have maxima d_{50} 3.4 μm ($YFe_{0.95}In_{0.05}O_{3\pm\delta}$) and 3.8 μm ($YFe_{0.95}Ga_{0.05}O_{3\pm\delta}$). The difference between both samples is apparent especially for the highest temperature of firing where the d_{90} value of Ga^{3+} pigments is twice that of In^{3+} doped ones.

CONCLUSIONS

Pigments of type $YFeO_{3\pm\delta}$ doped with 5 mol. % of Ga^{3+} or In^{3+} ions were prepared by mechanical activation in liquid medium and applied in an organic matrix and a ceramic glaze. Using TG-DTA analysis it was found that the perovskite phase is formed in the temperature range 900 - 982°C and that there are differences between the classical ceramic method of synthesis and mechanical activation. X-ray diffraction analysis confirmed the formation of $YFeO_3$ and $Y_3Fe_5O_{12}$. The standard pigment and the pigment doped with Ga^{3+} ions were fully reacted at 1200°C. Doping with In^{3+} ions was proved to be less suitable because they have bigger ionic radius than Fe^{3+} ions, which caused bad incorporation of these ions into the perovskite structure. The color of the samples is changing from red to dark yellowish brown in the case of a mass tone, from pink to light brown in a diluted tone. Doping with Ga^{3+} or In^{3+} ions caused an increase of the red and yellow tint of the samples. The ceramic glaze is reddish brown and the calcination temperature or the composition does not have a significant effect on the resulting hue. The median particle size is ranging from 1 to 6 μm which is size suitable for application of these pigments in various kinds of binders.

Acknowledgement

This work has been supported by University of Pardubice under the project SGS_2016_014.

REFERENCES

1. Forestier H., Guit-Guillain G. (1950): Etude thermomagnétique des ferrites de dysprosium et d'erbium. *Comptes Rendus de l'Académie des Sciences*, *239*, 155-157.
2. Krishnan R., Lisfi A., Guyot M., Cagan V. (1995): Preparation and some properties of pulsed laser deposited $YFeO_3$ films. *Journal of Magnetism and Magnetic Materials*, *147*, L221-L224. doi:10.1016/0304-8853(95)00302-9
3. Racu A.V., Ursu D.H., Kuliukova O.V., Logofatu C., Leca A., Miclau M. (2015): Direct low temperature hydrothermal synthesis of $YFeO_3$ microcrystals. *Materials Letters*, *140*, 107–110. doi:10.1016/j.matlet.2014.10.129.

4. Markova-Velichkova M., Lazarova T., Tumbalev V., Ivanov G., Kovacheva D., Stefanov P., Naydenov A. (2013): Complete oxidation of hydrocarbons on $YFeO_3$ and $LaFeO_3$ catalysts. *Chemical Engineering Journal*, *231*, 236–244. doi:10.1016/j.cej.2013.07.029
5. Tanaka H., Mizuno N., Misono M. (2003): Catalytic activity and structural stability of $La_{0.9}Ce_{0.1}Co_{1-x}Fe_xO_3$ perovskite catalysts for automotive emissions control. *Applied Catalysis A: General*, *244*, 371–382. doi:10.1016/S0926-860X(02)00609-9
6. Zhang Y., Yang J., Xu J., Gao Q., Hong Z. (2012): Controllable synthesis of hexagonal and orthorhombic $YFeO_3$ and their visible-light photocatalytic activities. *Materials Letters*, *81*, 1–4. doi:10.1016/j.matlet.2012.04.080
7. Stevens F., Cloots R., Poelman D., Vertruyen B., Henrist C. (2014): Low temperature crystallization of yttrium orthoferrite by organic acid-assisted sol–gel synthesis. *Materials Letters*, *114*, 136–139. doi:10.1016/j.matlet.2013. 09.108
8. Bamzai K., Razdan A.K., Kotru P.N. (1992): Dislocation etchants for flux grown $YFeO_3$ single crystals. *Journal of Crystal Growth*, *121*, 519–521. doi:10.1016/0022-0248(92)90164-E
9. Abou-Sekkina M.M., EI-Kersh M.M., Shalma O.A. (1999): Thermophysical properties of gamma-irradiated $LaFeO_3$ and $YFeO_3$ orthoferrites. *Journal of Radioanalytical and Nuclear Chemistry*, *241*, 15-24. doi:10.1007/BF02347284
10. Gi D.M., Navarro M.C., Lagarrigue M.C., Guimpel J., Carbonio R.E., Gómez M.I. (2011): Synthesis and structural characterization of perovskite $YFeO_3$ by thermal decomposition of a cyano complex precursor, $Y[Fe(CN)_6]_4H_2O$. *Journal of Thermal Analysis and Calorimetry*, *103*, 889–896. doi:10.1007/s10973-010-1176-z.
11. Zhang W., Fang C., Yin W., Zeng Y. (2013): One-step synthesis of yttrium orthoferrite nanocrystals via sol–gel auto-combustion and their structural and magnetic characteristics. *Materials Chemistry and Physics*, *137*, 877-883. doi:10.1016/j.matchemphys.2012.10.029.
12. Tang P., Chen H., Cao F., Pan G. (2011): Magnetically recoverable and visible-light-driven nanocrystalline $YFeO_3$ photocatalysts. *Catalysis Science & Technology*, *1*, 1145–1148. doi:10.1039/c1cy00199j.
13. Mathur S., Veith M., Rapalaviciute R., Shen H., Goya G.F., Filho W.L.M., Berquo T.S. (2004): Molecule Derived Synthesis of Nanocrystalline $YFeO_3$ and Investigations on Its Weak Ferromagnetic Behavior. *Chemistry of Materials*, *16*, 1906-1913. doi:10.1021/cm0311729.
14. Sundarayya Y., Mandal P., Sundaresan A., Rao C.N.R. (2011): Mössbauer spectroscopic study of spin reorientation in Mn-substituted yttrium orthoferrite. *Journal of Physics: Condensed Matter*, *23*, 436001 (7pp). doi:10.1088/0953-8984/23/43/436001.
15. Wu L., Yu J. C., Zhang L., Wang X., Li S. (2004): Selective self-propagating combustion synthesis of hexagonal and orthorhombic nanocrystalline yttrium iron oxide. *Journal of Solid State Chemistry*, *177*, 3666–3674. doi: 10.1016/j.jssc.2004.06.020.
16. Downie L.J., Goff R.J., Kockelmann W., Forder S.D., Parker J.E., Morrison F.D., Lightfoot P. (2012): Structural, magnetic and electrical properties of the hexagonal ferrites $MFeO_3$ (M=Y, Yb, In). *Journal of Solid State Chemistry*, *190*, 52–60. doi:10.1016/j.jssc.2012.02.004.
17. Berbenni V., Milanese C., Bruni G., Girella A., Marini A. (2011): Synthesis of $YFeO_3$ by thermal decomposition of mechanically activated mixtures $Y(CH_3COO)_3{\cdot}4H_2O$–$FeC_2O_4{\cdot}2H_2O$. *Thermochimica Acta*, *521*, 218–223. doi:10.1016/j.tca.2011.04.028.
18. Shen T., Hu C., Yang W. L., Liu H. C., Wei X. L. (2015): Theoretical investigation of magnetic, electronic and optical properties of orthorhombic $YFeO_3$: A first-principle study. *Materials Science in Semiconductor Processing*, *34*, 114–120. doi:10.1016/j.mssp.2015.02.015.
19. Shen H., Xu J., Wu A. (2010): Preparation and characterization of perovskite $REFeO_3$ nanocrystalline powders. *Journal of Rare Earths*, *28*(3), 416 - 419. doi:10.1016/S1002-0721(09)60124-1.
20. Jiang L., Liu W., Wu A., Xu J., Liu Q., Luo L., Zhang H. (2012): Rapid synthesis of $DyFeO_3$ nanopowders by auto-combustion of carboxylate-based gels. *Journal of Sol-Gel Science and Technology*, *61*, 527–533. doi:10.1007/s10971-011-2655-9.
21. Ma Y., Chen X. M., Lin Y. Q. (2008): Relaxorlike dielectric behavior and weak ferromagnetism in $YFeO_3$ ceramics. *Journal of Applied Physics*, *103*, 124111. doi: 10.1063/1.2947601.
22. Han A., Ye M., Zhao M., Liao J., Wu T. (2013): Crystal structure, chromatic and near-infrared reflective properties of iron doped $YMnO_3$ compounds as colored cool pigments. *Dyes and Pigments*, *99*, 527-530. doi:10.1016/j.dyepig.2013.06.016.
23. Buxbaum G., Pfaff G. (2005). Industrial Inorganic Pigments. in: *Colorimetry. Third, Completely Revised Edition*, WILEY-VCH Verlag GmbH & Co. KGaA. pp. 23–27.
24. Adachi G., Imanaka N., Kang Z.C. (2004). *Binary Rare Earth Oxides*. Kluwer Academic Publishers.
25. Šubrt J., Vinš J., Zapletal V., Balek V., Šaplygin I. S. (1988): Reactivity of finely dispersed iron (III) oxides and oxide hydroxides in solid-state reactions. *Journal of Thermal Analysis*, *33*, 455-461. doi:10.1007/BF01913923
26. Kytayama K., Sakaguchi M., Takahara Y., Endo H., Ueki H. (2004): Phase equilibrium in the system Y–Fe–O at 1100 °C. *Journal of Solid State Chemistry*, *177*, 1933–1938. doi:10.1016/j.jssc.2003.12.040.
27. Joint Committee on Powder Diffraction Standards, International Centre of Diffraction Data, Swarthmore, PA, USA, 1975.